

Polarimetric SAR Observation in Non-Spherical Rain Drop Environments

[#]Hiroaki Yasuma ¹ and Hajime Fukuchi ¹

¹Department of Aerospace Engineering, Tokyo Metropolitan University
Asahigaoka 6-6, Hino, Tokyo 191-0065, Japan, fuku@tmu.ac.jp

1. Introduction

There are various spaceborne SARs in operation now. It is expected that high-frequency and high-resolution SARs will become successful in the future. On the other hand, the influence of rain on measurement cannot be ignored, especially in the case of intense rain as the observation frequency increases[1]. Evaluation of these influences becomes an important issue for the accurate polarimetric SAR observation. The purpose of this paper is to consider the radio wave of polarimetric SAR propagation in rain and to verify the influence of the rainfall quantitatively.

2. Radio Wave Propagation in Rain

For a common monostatic polarimetric SAR system in the antenna coordinate system, the measured scattering matrix, \mathbf{M} , can be written as;

$$\mathbf{M} = \mathbf{R}'\mathbf{F}\mathbf{P}\mathbf{Q}\mathbf{S}\mathbf{Q}\mathbf{P}\mathbf{T} + \mathbf{N} \quad (1)$$

where \mathbf{R} is the receiving antenna distortion matrix, \mathbf{F} represents the one-way Faraday rotation matrix, \mathbf{P} is the ice distortion matrix, \mathbf{Q} is the rain distortion matrix, \mathbf{S} is the scattering matrix of the target, \mathbf{T} is the transmitting antenna distortion matrix, and \mathbf{N} represents additive noise terms present in each measurement due to earth radiation, thermal fluctuations in the receiver, digitization noise, and so on.

In this paper, we assume that the SAR system is ideal, and the rainfall is only a cause of the measurement error source. The radio wave is absorbed and scattered by rain drops in the range where the radio wave is irradiated. In addition, rain drops those are the same distance from SAR to the observation target point of land surface affect the SAR measurement as backscattering phenomena, and those are considered to be incoherent signals. Assuming that they only contribute to an increase in the noise terms, and the total amount of noise, \mathbf{N} , is negligible, (1) can be written

$$\mathbf{M} = \mathbf{Q}\mathbf{S}\mathbf{Q} \quad (2)$$

or

$$\begin{pmatrix} M_{HH} & M_{HV} \\ M_{VH} & M_{VV} \end{pmatrix} = \begin{pmatrix} Q_{HH} & Q_{HV} \\ Q_{VH} & Q_{VV} \end{pmatrix} \begin{pmatrix} S_{HH} & S_{HV} \\ S_{VH} & S_{VV} \end{pmatrix} \begin{pmatrix} Q_{HH} & Q_{HV} \\ Q_{VH} & Q_{VV} \end{pmatrix} \quad (3)$$

Now if \mathbf{Q} is computable with already-known \mathbf{S} , measured matrix influenced by raindrops, \mathbf{M} can be obtained.

3. Rain Distortion Matrix

Next, we calculate the elements of the rain distortion matrix, \mathbf{Q} , by using the method in reference[2]. In this method, the elements of \mathbf{Q} are given by

$$\begin{aligned} Q_{HH} &= e^{\lambda_1 L} \cos^2 \theta \cdot (1 + G \tan^2 \theta) \\ Q_{HV} &= Q_{VH} = e^{\lambda_1 L} \cos^2 \theta \cdot (1 - G) \tan \theta \\ Q_{VV} &= e^{\lambda_1 L} \cos^2 \theta \cdot (G + \tan^2 \theta) \end{aligned} \quad (4)$$

where

$$G = e^{(\lambda_1 - \lambda_2)L} \quad (5)$$

θ is the average canting angles of the rain drops, L is the rain area length, and eigenvalues λ_1 and λ_2 are given by

$$\left. \begin{matrix} \lambda_1 \\ \lambda_2 \end{matrix} \right\} = -jk_0 - jk_z \left[\frac{1 - e^{-2\sigma'^2} \cdot \cos 2\gamma}{2} \right] - \frac{j}{2} \left[\frac{1 + e^{-2\sigma'^2} \cdot \cos 2\gamma}{2} \right] \cdot \left[(k_x + k_y) \pm (k_x - k_y) e^{e^{-2\sigma'^2}} \right] \quad (6)$$

$$\lambda_1 - \lambda_2 = -j \left[\frac{1 + e^{-2\sigma'^2} \cdot \cos 2\gamma}{2} \right] \cdot \left[(k_x - k_y) e^{e^{-2\sigma'^2}} \right] \quad (7)$$

where σ is the standard deviation of θ , and σ' is that of γ , the average elevation angles. The parameters k_x , k_y and k_z , which give the propagation constants for respective polarizations, and k_0 , which gives the free-space wavenumber, are defined by

$$\begin{aligned} k_x &= \frac{2\pi}{k_0} \int f_x(a_0, 0) \cdot N(a_0) \cdot da_0 \\ k_y &= \frac{2\pi}{k_0} \int f_y(a_0, 0) \cdot N(a_0) \cdot da_0 \\ k_z &= \frac{2\pi}{k_0} \int f_x\left(a_0, \frac{\pi}{2}\right) \cdot N(a_0) \cdot da_0 = \frac{2\pi}{k_0} \int f_y\left(a_0, \frac{\pi}{2}\right) \cdot N(a_0) \cdot da_0 \end{aligned} \quad (8)$$

where a_0 is the rain drop effective radius, $N(a_0)$ is the drop size distribution, and $f_{x,y}(a_0, \gamma)$ is the forward scattering amplitudes when the elevation angle is γ .

4. Estimation Results

Now we can calculate \mathbf{Q} by using (4)-(8). $|Q_{HH}|$ is the amount of rain attenuation of horizontal polarization along one-way propagation path. Rain attenuation of C, X, and Ku bands are shown in Fig. 1.

$|Q_{VV} / Q_{HH}|$ corresponds to the attenuation difference of the horizontal polarization and the vertical one. When the radio waves enter into the rain drop, the horizontal polarization is attenuated more greatly than the vertical polarization because of the non-spherical rain drop shape as shown in

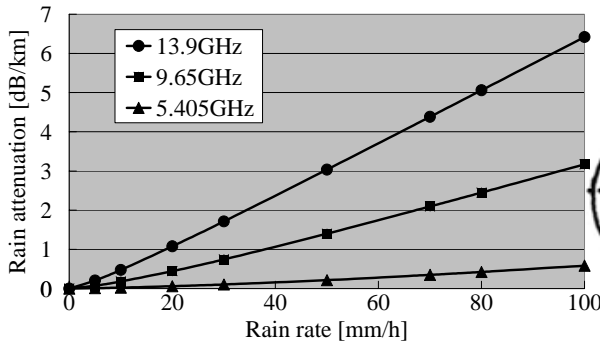


Fig. 1. Specific Rain Attenuation (horizontal pol.)

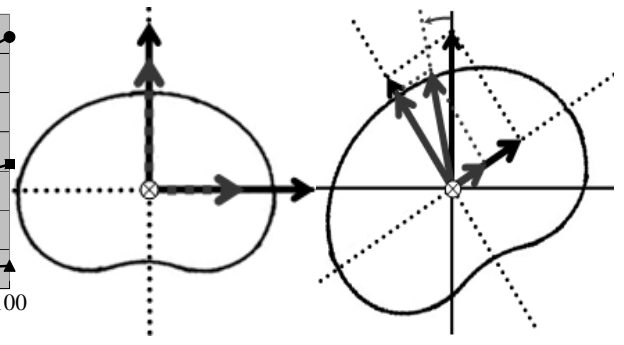


Fig. 2. Attenuation in a rain drop

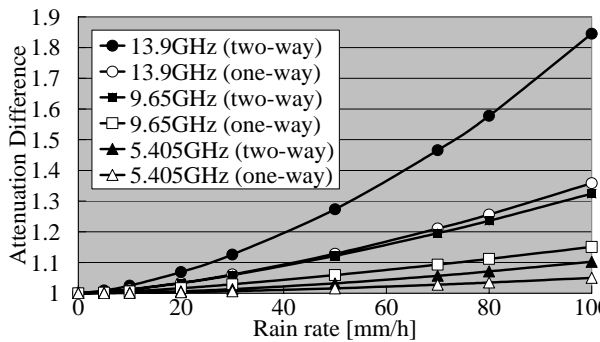


Fig. 3. Attenuation Difference ($\theta=0^\circ$)

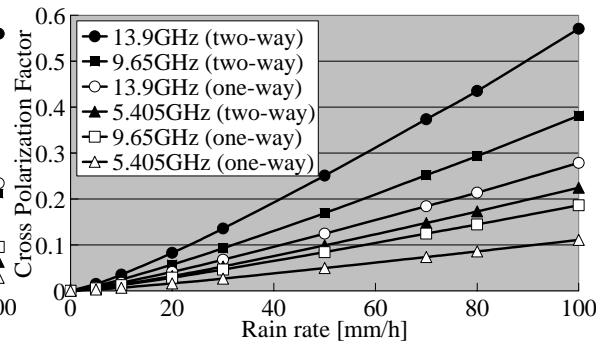


Fig. 4. Cross Polarization Factor ($\theta=45^\circ$)

Fig. 2 on the left-hand side. Moreover, if the rain drops incline with a certain canting angle, depolarization will occur as seen in Fig. 2 on the right-hand side.

$|Q_{HV} / Q_{HH}|$ shows amplitude of this depolarization. We estimate the attenuation difference ($|Q_{VV} / Q_{HH}|$) and the depolarization ($|Q_{HV} / Q_{HH}|$) as a function of rainfall rate. The estimated results are shown in Fig. 3 and Fig. 4, provided that \mathbf{S} is unit matrix, L is 5km, γ is 50° , θ is 0° or 45° , and Marshall-Palmer drop size distribution is assumed.

The estimated results can be expressed by polarization signatures as in Fig. 5 to Fig. 16, provided that the rainfall rate is 50mm/h, θ is 22.5° , and the observation frequency is 9.65 GHz. The scattering property of \mathbf{S} was assumed to be three kinds of reflectors, i.e. Plate, Twist, and Dihedral, and those scattering matrices are $\begin{bmatrix} 1 & 0 \\ 0 & 1 \end{bmatrix}$, $\begin{bmatrix} 0 & 1 \\ 1 & 0 \end{bmatrix}$, and $\begin{bmatrix} 1 & 0 \\ 0 & -1 \end{bmatrix}$ respectively. These figures show that rain gives the major effect to polarimetric SAR observation especially in a high frequency like X band.

5. Conclusions

The rain effect on polarimetric SAR observation was quantitatively evaluated by using the SAR observation model in non-spherical rain drop environments.

References

- [1] A. Dankmayer, Bjorn J. Doring, Marco Schwerdt, and Madhu Chandra, "Assessment of Atmospheric Propagation Effects in SAR Images," *IEEE Trans. Geosci. Remote Sensing*, vol. 47, pp. 3507-3518, 2009.
- [2] Tomohiro Oguchi, "Scattering properties of Pruppacher-and-Pitter form rain drops and cross polarization due to rain: Calculation at 11, 13, 19.3 and 34.8GHz," *Radio Science*, vol. 12, no. 1, pp. 41-51, 1977.

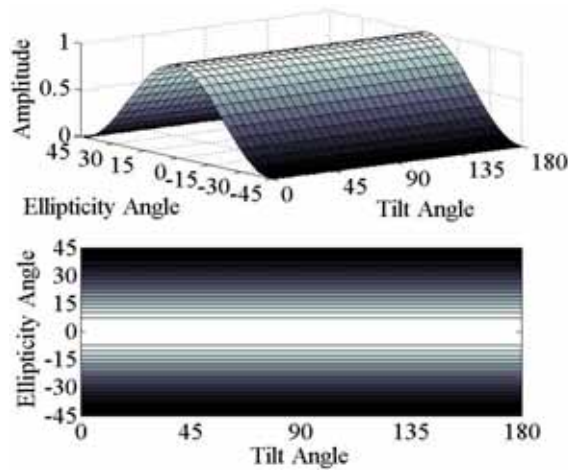


Fig. 5. Co-pol. signature (Plate, ideal)

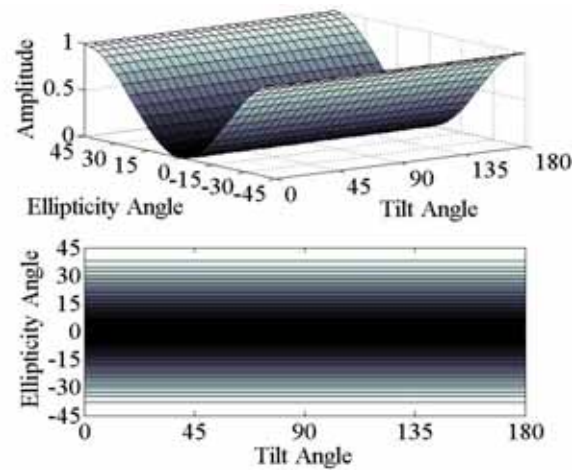


Fig. 6. Cross pol. signature (Plate, ideal)

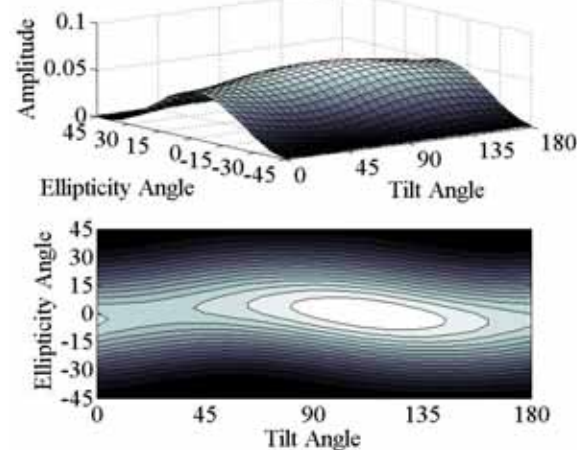


Fig. 7. Co-pol. (Plate, 9.65GHz, $R=50\text{mm/h}$)

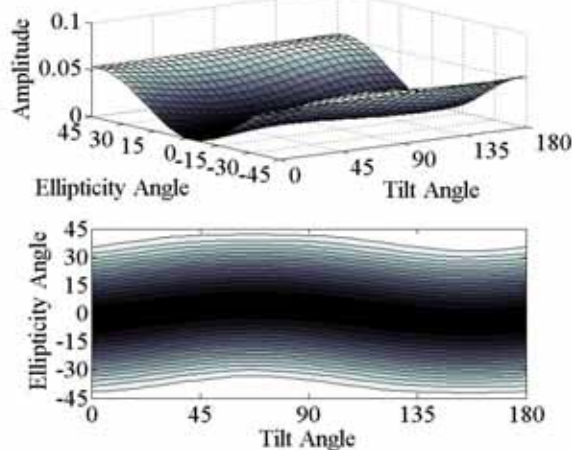


Fig. 8. Cross pol. (Plate, 9.65GHz, $R=50\text{mm/h}$)

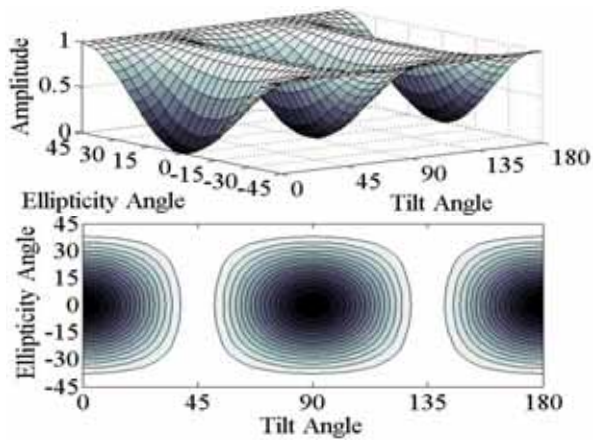


Fig. 9. Co-pol. signature (Twist, ideal)

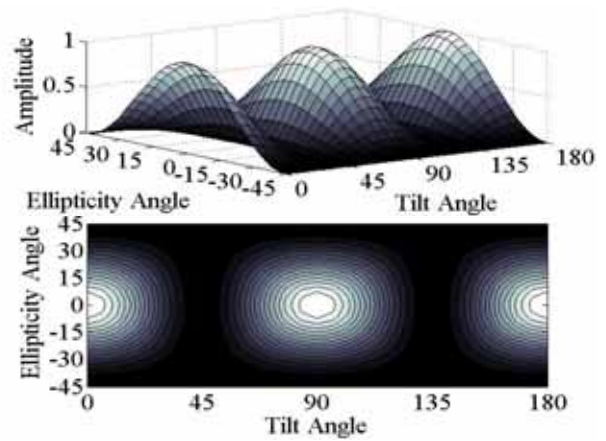


Fig. 10. Cross pol. signature (Twist, ideal)

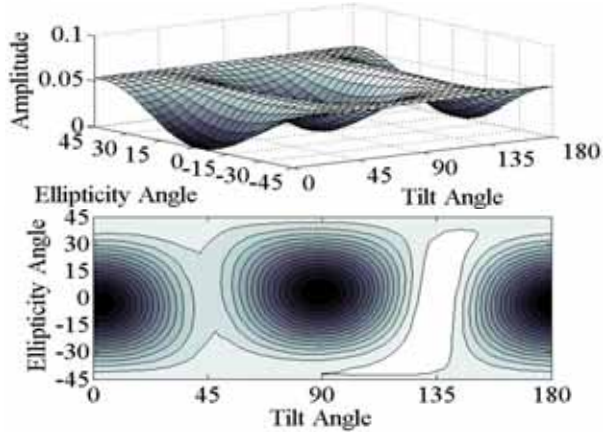


Fig. 11. Co-pol. (Twist, 9.65GHz, $R=50\text{mm/h}$)

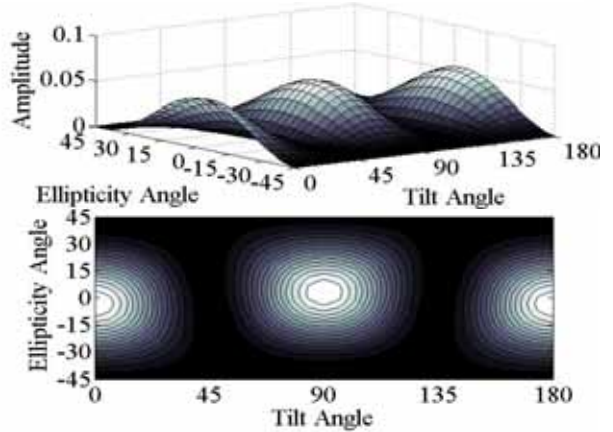


Fig. 12. Cross pol. (Twist, 9.65GHz, $R=50\text{mm/h}$)

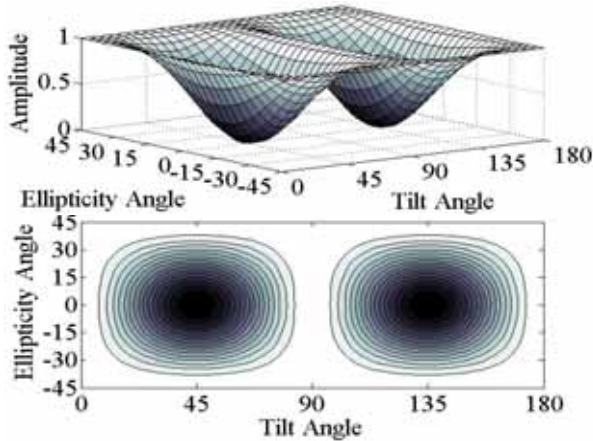


Fig. 13. Co-pol. signature (Dihedral, ideal)

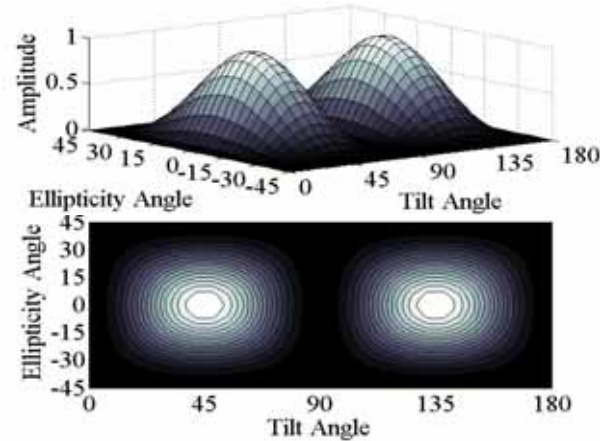


Fig. 14. Cross pol. signature (Dihedral, ideal)

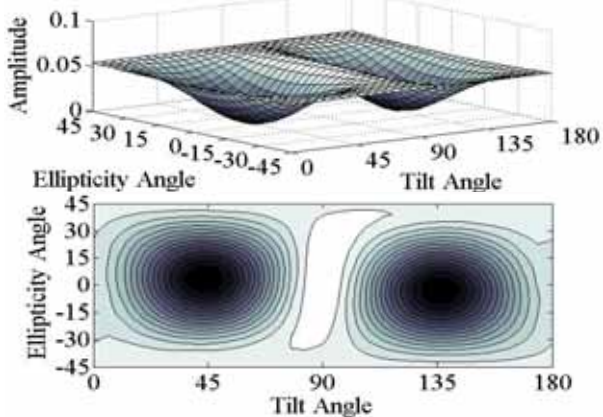


Fig. 15. Co-pol. (Dihedral, 9.65GHz, $R=50\text{mm/h}$)

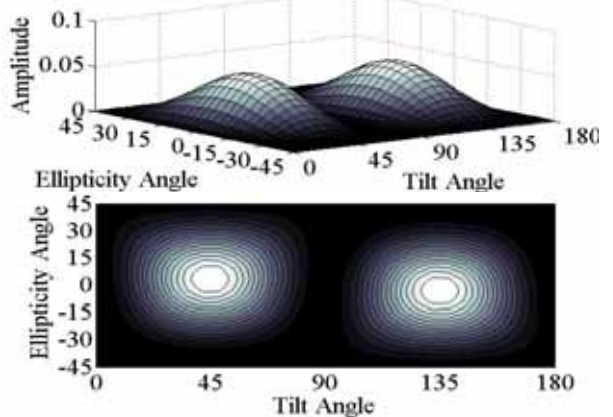


Fig. 16. Cross pol. (Dihedral, 9.65GHz, $R=50\text{mm/h}$)